The Influence of the Spatial Heterogeneity of Vegetation Cover and Surface Topography on Vertical CO_2 Fluxes within the Atmospheric Surface Layer

A. V. Olchev[a, b], *, Yu. V. Mukhartova[b], **, N. T. Levashova[b], *, E. M. Volkova[c],
M. S. Ryzhova[b], and P. A. Mangura[b]**

[a]*Severtsov Institute of Ecology and Evolution, Russian Academy of Sciences, Moscow, 119071 Russia*
[b]*Moscow State University, Moscow, 119991 Russia*
[c]*Tula State University, Tula, 300012 Russia*
*e-mail: aoltche@gmail.com
**e-mail: muhartova@yandex.ru
***e-mail: convallaria@mail.ru

Abstract—The influence of the spatial heterogeneity of vegetation cover and topography on CO_2 fluxes in the atmospheric surface layer is estimated using a two-dimensional (2D) hydrodynamic model of turbulent exchange. A ~4.5-km-long profile that crossed a hilly area with a mosaic vegetation cover in Tula region was selected for model experiments. During the first experiment, a wind field and vertical fluxes were calculated by the 2D model for the entire selected profile with respect to the horizontal heterogeneity of the vegetation cover and surface topography. In the second experiment, the profile was considered an assemblage of elementary independent homogeneous segments; for each of them, vertical fluxes were calculated by the 2D model with the assumption of 'zero' horizontal advection, i.e., the required functions are independent of the horizontal coordinates. The influences of any boundary effects that appear at the interface between the different vegetation communities and at topographical irregularities on the turbulent regime are ignored in this case. For the profile selected, ignoring the horizontal advection, disturbances in the wind field that appeared at surface topography irregularities, and boundaries between different vegetation communities can lead to a 26% underestimation of the total CO_2 absorption by the ground surface on a clear sunny day under summer weather conditions.

Keywords: CO_2 flow, turbulent exchange, two-dimensional hydrodynamic model, heterogeneous vegetation, surface topography, atmospheric surface layer

DOI: 10.1134/S0001433817050103

The problem of an appropriate estimation of vertical turbulent fluxes of greenhouse gases between a horizontally heterogeneous ground surface, covered by the forest and meadow vegetation, and the atmosphere is extremely important, primarily due to the key role of forests in the balance of greenhouse gases in the atmosphere and their influence on the climate system. The disturbances in the wind field and in the turbulent regime that appear due to interaction of the air flow with roughness elements (crowns of trees, forest edges, clearings in a forest, clear-cuts, windthrows, topographical irregularities, etc.) significantly restrict the possibilities of using not only classical experimental approaches for the definition of sensible heat, CO_2 and H_2O fluxes (the eddy covariance method [1–5]), but also using the most widespread one-dimensional (1D) model approaches based on the assumption about horizontal homogeneity of the land surface [6–8]. It is evi-

dent that, to describe the exchange processes in the atmospheric surface layer over the heterogeneous surface, the more complex two- and three-dimensional (2D and 3D) models of turbulent exchange can serve as the most effective instruments, which make it possible to calculate not only vertical but also horizontal fluxes with respect to the actual structure of the vegetation cover and surface topography.

Most of the existed 2D and 3D models are based on solving the system of two differential equations: a Navier–Stokes vector equation and a scalar equation of continuity [9–12]. The equations are solved relative to three components of the wind vector and atmosphere pressure using the Reynolds averaging. Further, for the closure of the system of equations, the different methods are used, among which the approaches based on the Boussinesq hypothesis [13] are the most widely used. According to this hypothesis, a tensor of
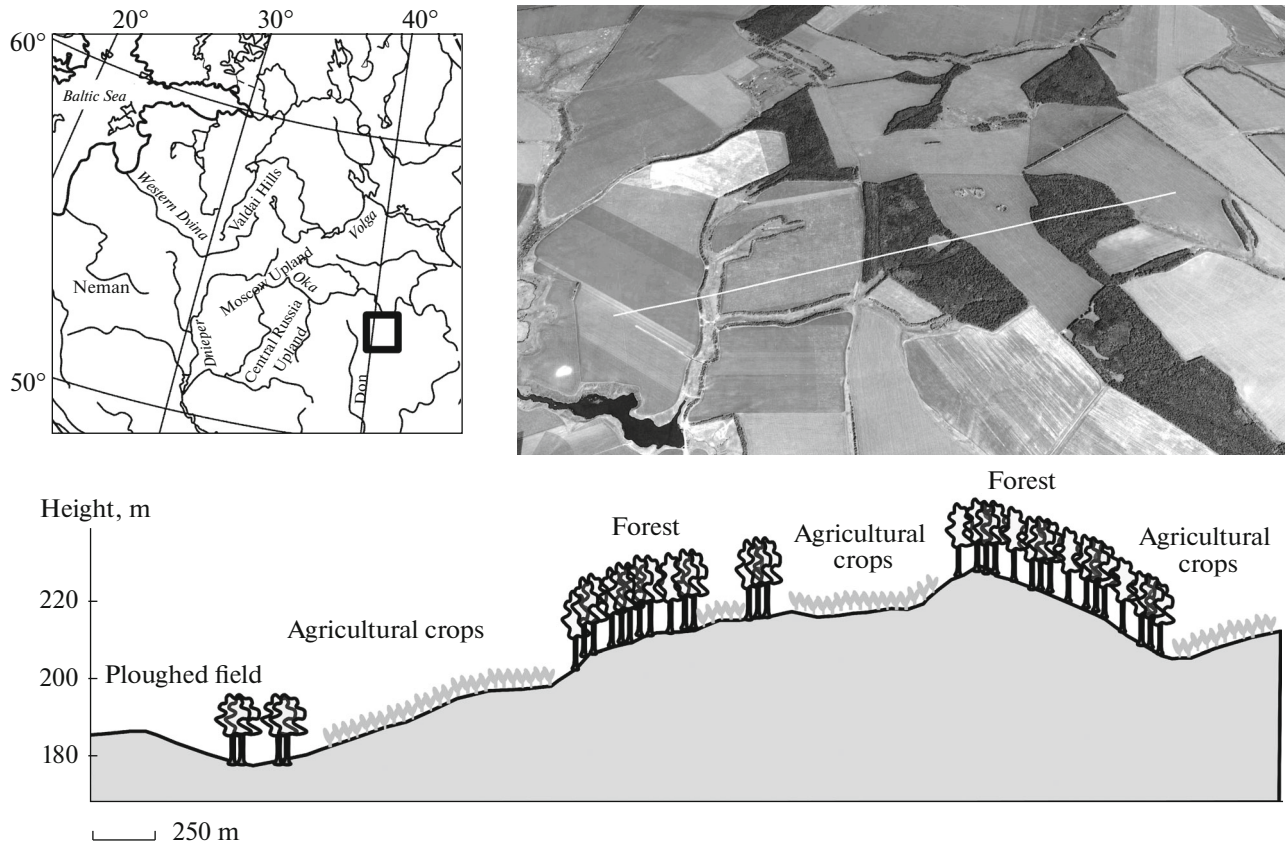
Fig. 1. Geographical location, satellite image, and vegetation and topography along the 4.5-km profile selected for numerical experiments. The profile is shown by a white line in the satellite image.

turbulent stresses can be determined similarly to the tensor of viscous stresses through gradients from the averaged wind velocity field [14].

The main idea of this study is to develop and apply a 2D model of the turbulent exchange for describing the CO_2 transfer above the heterogeneous land surface with a mosaic vegetation cover and a complex topography, as well as for estimating possible errors of calculating vertical turbulent CO_2 fluxes in case of neglecting horizontal advection and disturbances that appear in the wind field at topographic irregularities and boundaries between different vegetation communities accepted in 1D models.

MATERIALS AND METHODS

General Characteristics of the Study Area

To perform the model experiments, we selected a small area bounded by the geographical coordinates 53°39′ and 53°42′ N, 38°28′ and 38°34′ E in the Kurkin region in the southeast of Tula oblast. It is located in the forest-steppe zone and is characterized by hilly topography with mosaic forest vegetation, agricultural crops, and steppe meadows (Fig. 1).

For the numerical experiments, a profile that crossed the selected area from southwest to northeast and corresponded to the prevailing wind direction in the region under study during the summer. The profile had a length of ~4.5 km; the maximum elevation difference reached 50 m. Most of the area adjacent to this profile is covered by agricultural crops (corn, spring wheat). The tree vegetation along the profile is represented primarily by oak and birch plantations and a well-pronounced shrub layer. The average height of woody species varies from 15 to 20 m. A few willow thickets grow along the slopes and at the bottoms of gullies, where ground waters come out. The grass vegetation is represented by steppe meadows mainly along the steep gully slopes.

A Two-Dimensional Hydrodynamic Model of Exchange

A two-dimensional hydrodynamic model of turbulent exchange is based on the solution of a system of the Navier–Stokes vector equation and the equation of continuity. The model uses the 1.5th order closure, which uses the Boussinesq hypothesis, as well as the expression of coefficients of turbulent diffusion (K, m^2 s^{-1}) as a function of the turbulent

kinetic energy (E, m^2 s^{-2}) and the rate of its dissipation (ε, m^2 s^{-3}) [14−16]:

$$K = C_\mu E^2 \varepsilon^{-1},$$

where C_μ is the dimensionless coefficient of proportionality.

The averaged system of equations for the horizontal (u, m s^{-1}) and vertical (w, m s^{-1}) components of the wind velocity $\vec{V} = \{u, w\}$ and excess kinematic pressure (δP, Pa) is written as [17]

$$\begin{cases} \dfrac{\partial u}{\partial t} + u\dfrac{\partial u}{\partial x} + w\dfrac{\partial u}{\partial z} = -\dfrac{1}{\rho_0}\dfrac{\partial \delta P}{\partial x} - \dfrac{2}{3}\dfrac{\partial E}{\partial x} \\ + \dfrac{\partial}{\partial x}\left(2K\dfrac{\partial u}{\partial x}\right) + \dfrac{\partial}{\partial z}\left(K\dfrac{\partial u}{\partial z}\right) + \dfrac{\partial}{\partial z}\left(K\dfrac{\partial w}{\partial x}\right) + F_u, \\ \dfrac{\partial w}{\partial t} + u\dfrac{\partial w}{\partial x} + w\dfrac{\partial w}{\partial z} = -\dfrac{1}{\rho_0}\dfrac{\partial \delta P}{\partial z} - \dfrac{2}{3}\dfrac{\partial E}{\partial z} \\ + \dfrac{\partial}{\partial z}\left(2K\dfrac{\partial w}{\partial z}\right) + \dfrac{\partial}{\partial x}\left(K\dfrac{\partial w}{\partial x}\right) + \dfrac{\partial}{\partial x}\left(K\dfrac{\partial u}{\partial z}\right) + F_w, \\ \dfrac{\partial u}{\partial x} + \dfrac{\partial w}{\partial z} = 0, \end{cases}$$

where ρ_0 is the air density, kg m^{-3}; F_u, F_w are the horizontal and vertical components of viscous drag force $\vec{F} = \{F_u, F_w\}$ that is accounted for the unit of mass and appears during the interaction of an air flow with elements of vegetation, m s^{-2} [18]. We calculate it as

$$\mathbf{F} = -c_d \cdot LAD \cdot |\mathbf{V}| \cdot \mathbf{V},$$

where LAD is the leaf area density, m^2 m^{-3}; c_d is the dimensionless coefficient of aerodynamic resistance of vegetation elements.

To calculate E and the rate of its dissipation ε, we use the system of differential equations written analogously with the equation of turbulent diffusion in a moving flow [19]:

$$\begin{cases} \dfrac{\partial E}{\partial t} + u\dfrac{\partial E}{\partial x} + w\dfrac{\partial E}{\partial z} = \dfrac{\partial}{\partial x}\left(\dfrac{K}{\sigma_E^\phi}\dfrac{\partial E}{\partial x}\right) \\ + \dfrac{\partial}{\partial z}\left(\dfrac{K}{\sigma_E^\phi}\dfrac{\partial E}{\partial z}\right) + P_E - \varepsilon, \\ \dfrac{\partial \phi}{\partial t} + u\dfrac{\partial \phi}{\partial x} + w\dfrac{\partial \phi}{\partial z} = \dfrac{\partial}{\partial x}\left(\dfrac{K}{\sigma_\phi}\dfrac{\partial \phi}{\partial x}\right) \\ + \dfrac{\partial}{\partial z}\left(\dfrac{K}{\sigma_\phi}\dfrac{\partial \phi}{\partial z}\right) + \dfrac{\phi}{E}(C_{\phi 1}P_E - C_{\phi 2}\varepsilon) + \Delta_\phi. \end{cases} \quad (1)$$

The second equation of system (1) is presented for the supplemented function $\phi = \varepsilon/E$ [s^{-1}] that characterizes the mixing length. The dimensionless values σ_E^ϕ and σ_ϕ ($\sigma_E^\phi = \sigma_\phi = 2$) represent the Prandlt number for the turbulent kinetic energy and the turbulent Schmidt number for the function ϕ, respectively. The

dimensionless coefficients $C_{\phi 1}$ ($C_{\phi 1} = 0.52$) and $C_{\phi 2}$ ($C_{\phi 2} = 0.8$) are model constants [20]. In a two-dimensional case, the shear production of the turbulent kinetic energy (P_E, m^2 s^{-3}) is expressed as [17]

$$P_E = 2K\left(\left(\dfrac{\partial u}{\partial x}\right)^2 + \left(\dfrac{\partial w}{\partial z}\right)^2\right) + K\left(\dfrac{\partial u}{\partial z} + \dfrac{\partial w}{\partial x}\right)^2.$$

The term Δ_ϕ [s^{-2}] in the second equation of system (1) describes an increase in dissipation of the turbulent kinetic energy due to the interaction of an air flow and vegetation and is expressed in the first approximation as [19, 21]

$$\Delta_\phi = 12\sqrt{C_\mu}(C_{\phi 2} - C_{\phi 1})c_d LAD|\mathbf{V}|\phi.$$

For the CO_2 concentration in the air flow, the advection-turbulent diffusion equation is written as [17]

$$\begin{aligned} &\dfrac{\partial C}{\partial t} + u\dfrac{\partial C}{\partial x} + w\dfrac{\partial C}{\partial z} \\ &= \dfrac{\partial}{\partial x}\left(K_C\dfrac{\partial C}{\partial x}\right) + \dfrac{\partial}{\partial z}\left(K_C\dfrac{\partial C}{\partial z}\right) + f_C, \end{aligned} \quad (2)$$

where C is the CO_2 concentration, μmol m^{-3}; K_C is the coefficient of turbulent diffusion for CO_2, m^2 s^{-1}; and f_C is the function describing the sources and sinks of CO_2 in the atmospheric surface layer (vegetation cover and soil), μmol m^{-3} s^{-1}.

For the calculation of K_C, we assume that it is proportional to K in the model [22]:

$$K_C = \dfrac{K}{Sc},$$

where Sc is the dimensionless turbulent Schmidt number [22, 23] that is taken as equal to 0.75 in our study.

For the vegetation cover, f_C is calculated as the difference of the CO_2 fluxes released in a unit volume by nonphotosynthesizing parts of plants (e.g. branches and stems of trees) due to respiration and CO_2 uptake by leaves of plants by photosynthesis:

$$f_C = SAD \cdot R_t - LAD \cdot A. \quad (3)$$

Here, SAD is the surface area of nonphotosynthesizing parts of plants in a unit volume, m^2 m^{-3}; R_t is the respiration rate of plants, μmol m^{-2} s^{-1}; and A is the net photosynthesis rate of photosynthesizing plant leaves, μmol m^{-2} s^{-1}.

The rate of net photosynthesis of plant leaves (A) is obtained in expression (3) according to the approach proposed by Ball et al. [24] and Leuning [25]:

$$A = \dfrac{1}{a_1}(g_s - g_0)(C_s - \Gamma_*)\left(1 + \dfrac{D_s}{D_0}\right),$$

where g_s is the stomatal conductance for CO_2, mol m^{-2} s^{-1}; g_0 is the value of g_s at a light compensation point ($g_0 = 0.008$ mol m^{-2} s^{-1}); Γ_* is the carbon dioxide compen-

sation point ($\Gamma_* = 18$ μmol CO_2 mol^{-1} of dry air); D_s is the deficit of water vapor pressure ($D_s = 10$ hPa); C_s is the CO_2 concentration in the air layer adjacent to the leaf surface (μmol CO_2 mol^{-1} of dry air) calculated from advection-turbulent diffusion equation (2) for CO_2; and a_1 and D_0 are empirical coefficients ($a_1 = 6$, $D_0 = 16.7$ hPa).

The value of R_t is estimated using the Arrhenius equation

$$R_t = R_{t,\mathrm{ref}} \exp\left[\frac{E_a(T_t - T_{\mathrm{ref}})}{T_{\mathrm{ref}} R T_t}\right],$$

where $R_{t,\mathrm{ref}}$ is the respiration rate of tree stems, μmol m^{-2} s^{-1}, at the temperature $T_{\mathrm{ref}} = 25°C$ (298.15 K); T_t is the vegetation surface temperature, K; E_a is the energy of activation that depends on the plant eco-physiological properties ($E_a = 24000$ J mol^{-1}), and R is the universal gas constant ($R = 8.314$ J K^{-1} mol^{-1}).

The stomatal conductance of leaves is calculated as a function of photosynthetically active radiation (G) coming into the leaf surface, μmol m^{-2} s^{-1} [26]:

$$g_s = g_{s\,\mathrm{max}} f(G),$$

where $g_{s\mathrm{max}}$ is the maximum possible value of g_s for the corresponding plant species, provided that all stomata are completely open, and $f(G)$ is the function describing the dependence of g_s on G:

$$f(G) = 1 - e^{-\beta G(z)},$$

where β is the empirical constant that characterizes an angle of slope of the photosynthetic light response curve at $G \to 0$, m^2 s μmol^{-1}, and $G(z)$ is the value of G at the level z inside the vegetation cover.

We assign the rate of CO_2 emission from the soil surface (R_s), μmol m^{-2} s^{-1}, as a lower boundary condition in the model. In the model calculations, we made an assumption on the R_s dependence on the temperature (based on the Arrhenius equation) and soil moisture, as well as on the wind velocity at the soil surface:

$$R_s = R_{s,\mathrm{ref}} \exp\left[\frac{E_a(T_s - T_{\mathrm{ref}})}{T_{\mathrm{ref}} R T_s}\right]$$
$$\times (1 - \exp(-1.6 W_s))^{1.25}$$
$$\times \begin{cases} \exp(0.2(u(z_0))); \\ u(z_0) > 0.1 \text{ m s}^{-1} \\ 1 - \exp(-18 \times (u(z_0))); \\ u(z_0) \le 0.1 \text{ m s}^{-1} \end{cases},$$

where $R_{s,\mathrm{ref}}$ is the CO_2 emission from the soil surface, μmol m^{-2} s^{-1}, at the temperature $T_{\mathrm{ref}} = 25°C$ (298.15 K), T_s is the soil temperature at a depth of 5 cm, K; E_a is the activation energy that depends on soil properties, J mol^{-1}; $u(z_0)$ is the wind velocity at a height of 30 cm above the soil surface, m s^{-1}; and W_s is the moisture of the upper soil horizon, unit fractions.

The R_s dependence on soil moisture and the wind velocity at the soil surface was obtained from the results of the field experiments by measuring the CO_2 emission from the soil surface using the surface chamber with a varying ventilation rate. It was assumed that CO_2 is formed in the soil by respiration of the plant roots and soil organisms, CO_2 transfers in the soil via molecular diffusion, and its concentration within the soil pores considerably exceeds the ambient concentration of CO_2 within the atmospheric surface layer. At the soil surface, the CO_2 flux is directly proportional to the difference in the CO_2 concentrations between the upper soil horizon and a air layer above the soil surface, as well as to the coefficient of turbulent diffusion at the soil surface. It was assumed that the CO_2 emission from the soil surface is equal to the respiration rate of plant roots and soil microorganisms only under some equilibrium wind velocity within the air layer near the soil surface. In the model calculations, the value of this equilibrium wind velocity at a height of 0.3 m was taken equal to 1 m s^{-1}. If the wind velocities are higher than the selected equilibrium value, the CO_2 emission from the soil surface intensifies (due to the expulsion of the CO_2-saturated air from the soil pores), and when the wind velocities are small, tending to zero, the CO_2 transport significantly decreases in the near-soil layer due to the dominance of molecular diffusion over the turbulent exchange compared to the rate of CO_2 soil emission under equilibrium conditions. Thus, CO_2 accumulates in soil pores and under certain conditions it can further return into the atmosphere or be chemically bounded and stored within the soil. The CO_2 dissolved in water can also be removed from the ecosystem with a surface runoff.

A CO_2 flux over the vegetation cover along the selected profiles (F_C), μmol m^{-2} s^{-1}, is calculated with a horizontal grid spacing of 10 m from modeled vertical profiles of C and K by the formula

$$F_C = -K_C \frac{\partial C}{\partial z}.$$

All input parameters of the model that are required for the calculations and describe the photosynthesis and respiration of agricultural crops, woody and herbaceous plants, as well as CO_2 emission from the soil surface, were determined during intensive field campaigns in the study region in the summer of 2013–2015. For the measurements we used a portable system that included the transparent measuring chamber connected with the infrared gas analyzer Li-840 (Li-Cor, USA). The closed 'static' measuring scheme was applied [4, 27]. The values of Γ_* and $g_{s\,\mathrm{max}}$ for woody species, meadow vegetation, and agricultural plants at different stages of ontogenesis were taken from the literature [28].

When solving the system of equations, we used a logarithmic distribution of the wind velocity with

height as initial conditions. The background equilibrium concentration of CO_2 (~380 ppm) was assigned at a height of 100 m above the ground surface. We used an adhesion condition at the lower boundary of the computational domain and a drift condition at the free boundary. The ground surface (impermeable obstacles) was modeled as a limit case of permeable obstacles with very big coefficient of aerodynamic resistance.

Difference Scheme

To solve the system of equations numerically, we used a finite-difference approach based on the scheme of splitting with respect to the processes [11, 17, 29].

We introduce a grid x_n, $n = 0,1,...,N$, $x_0 = -L$, $x_N = L$; z_m, $m = 0,1,...,M$, $z_0 = h_0$, $z_M = H$; $t_j = j\tau$, $j = 0,1,...,J$, into the computational domain $x \in [-L, L]$, $z \in [h_0, H]$. When we already know the required functions at the layer t_j, to obtain them at a new $(j+1)$th layer, we use a transition through the auxiliary layer in time. We add an intermediate layer $t_{j+1/2} = t_j + \tau/2$ and perform transition from layer j to layer $j+1$ in several steps.

Let us consider a system of equations for the components of the wind velocity and excess pressure. The transition between layers t_j and $t_{j+1/2}$ is done using the difference approximation of the system of equations

$$\begin{cases} \dfrac{1}{2}\dfrac{\partial u}{\partial t} + u\dfrac{\partial u}{\partial x} + w\dfrac{\partial u}{\partial z} = \dfrac{\partial}{\partial x}\left(2K\dfrac{\partial u}{\partial x}\right) \\[2mm] + \dfrac{\partial}{\partial z}\left(K\dfrac{\partial u}{\partial z}\right) + \dfrac{\partial}{\partial z}\left(K\dfrac{\partial w}{\partial x}\right) - c_d LAD\sqrt{u^2 + w^2}\,u, \\[2mm] \dfrac{1}{2}\dfrac{\partial w}{\partial t} + u\dfrac{\partial w}{\partial x} + w\dfrac{\partial w}{\partial z} = \dfrac{\partial}{\partial x}\left(K\dfrac{\partial w}{\partial x}\right) \\[2mm] + \dfrac{\partial}{\partial z}\left(2K\dfrac{\partial w}{\partial z}\right) + \dfrac{\partial}{\partial x}\left(K\dfrac{\partial u}{\partial z}\right) - c_d LAD\sqrt{u^2 + w^2}\,w, \end{cases} \quad (4)$$

and the transition between the layers $t_{j+1/2}$ and t_{j+1} is done using the difference approximation of the system of equations

$$\begin{cases} \dfrac{1}{2}\dfrac{\partial u}{\partial t} = -\dfrac{\partial}{\partial x}\left(\dfrac{\delta P}{\rho_0} + \dfrac{2}{3}E\right), \\[3mm] \dfrac{1}{2}\dfrac{\partial w}{\partial t} = -\dfrac{\partial}{\partial z}\left(\dfrac{\delta P}{\rho_0} + \dfrac{2}{3}E\right), \end{cases} \quad (5)$$

assuming that the components of the wind velocity have already been found at $t_{j+1/2}$. Here, we consider that the equation of continuity is fulfilled for the velocity components at an integer layer.

To solve system of equations (4) at $t \in (t_j, t_{j+1/2}]$, we use a locally one-dimensional scheme [30, 31]. We introduce another intermediate later $t_{j+1/4} = t_j + \tau/4$ and split the system into two auxiliary systems:

$$\begin{cases} \dfrac{1}{4}\dfrac{\partial u}{\partial t} + u\dfrac{\partial u}{\partial x} = \dfrac{\partial}{\partial x}\left(2K\dfrac{\partial u}{\partial x}\right) + \dfrac{\partial}{\partial z}\left(K\dfrac{\partial w}{\partial x}\right) \\[2mm] - c_d LAD\sqrt{u^2 + w^2}\,u, \\[2mm] \dfrac{1}{4}\dfrac{\partial w}{\partial t} + u\dfrac{\partial w}{\partial x} = \dfrac{\partial}{\partial x}\left(K\dfrac{\partial w}{\partial x}\right) + \dfrac{\partial}{\partial x}\left(K\dfrac{\partial u}{\partial z}\right) \\[2mm] - c_d LAD\sqrt{u^2 + w^2}\,w, \end{cases} \quad t \in (t_j, t_{j+1/4}], \quad (6)$$

$$\begin{cases} \dfrac{1}{4}\dfrac{\partial u}{\partial t} + w\dfrac{\partial u}{\partial z} = \dfrac{\partial}{\partial z}\left(K\dfrac{\partial u}{\partial z}\right), \\[2mm] \dfrac{1}{4}\dfrac{\partial w}{\partial t} + w\dfrac{\partial w}{\partial z} = \dfrac{\partial}{\partial z}\left(2K\dfrac{\partial w}{\partial z}\right), \end{cases} \quad t \in (t_{j+1/4}, t_{j+1/2}].$$

Each equation in the auxiliary systems is approximated by unconditionally stable implicit schemes taking into account a sign of the multipliers u and w in the terms that are responsible for the transfer and contain the first derivatives of the functions u and w with respect to the spatial variables x and z. For example, for Eq. (6) we obtain,

$$\dfrac{u_{n,m}^{j+1/4} - u_{n,m}^{j}}{\tau} + u_{n,m}^{j}\,\mathrm{sgn}\left(u_{n,m}^{j}\right)\dfrac{u_{n,m}^{j+1/4} - u_{n-1,m}^{j+1/4}}{x_n - x_{n-1}}$$

$$+ u_{n,m}^{j}\left(1 - \mathrm{sgn}\left(u_{n,m}^{j}\right)\right)\dfrac{u_{n+1,m}^{j+1/4} - u_{n,m}^{j+1/4}}{x_{n+1} - x_n}$$

$$= 2L_{xx}\left[u^{j+1/4}\right] + L_{zx}\left[w^{j}\right]$$

$$- c_d LAD_{n,m}\sqrt{\left(u_{n,m}^{j}\right)^2 + \left(w_{n,m}^{j}\right)^2}\,u_{n,m}^{j+1/4},$$

where we used the designations $u_{n,m}^{j} = u\left(x_n, z_m, t_j\right)$, $u_{n,m}^{j+1/4} = u\left(x_n, z_m, t_j + \tau/4\right)$, $w_{n,m}^{j} = w\left(x_n, z_m, t_j\right)$, $LAD_{n,m} = LAD\left(x_n, z_m\right)$,

$$L_{xx}\left[u^{j+1/4}\right] = \frac{2}{x_{n+1} - x_{n-1}}$$

$$\times \left(K_{n+1/2,m}^{j} \frac{u_{n+1,m}^{j+1/4} - u_{n,m}^{j+1/4}}{x_{n+1} - x_n} - K_{n-1/2,m}^{j} \frac{u_{n,m}^{j+1/4} - u_{n-1,m}^{j+1/4}}{x_n - x_{n-1}} \right),$$

$$L_{zx}\left[w^j\right] = \frac{1}{z_{m+1} - z_{m-1}}$$

$$\times \left(K_{n,m+1}^{j} \frac{w_{n+1,m+1}^{j} - w_{n-1,m+1}^{j}}{x_{n+1} - x_{n-1}} - K_{n,m-1}^{j} \frac{w_{n+1,m-1}^{j} - w_{n-1,m-1}^{j}}{x_{n+1} - x_{n-1}} \right),$$

$$K_{n\pm1/2,m}^{j} = 0.5\left(K_{n\pm1,m}^{j} + K_{n,m}^{j} \right),$$

$$K_{n,m\pm1/2}^{j} = 0.5\left(K_{n,m\pm1}^{j} + K_{n,m}^{j} \right),$$

$$\mathrm{sgn}\left(u_{n,m}^{j}\right) = \begin{bmatrix} 1, u_{n,m}^{j} \geq 0, \\ 0, u_{n,m}^{j} < 0. \end{bmatrix}$$

Since the considered auxiliary equations for functions u and w have a similar structure to the equations for the functions E, φ and C, we use a similar scheme for solving these equations for these functions, the only difference being the transition from layer j to layer $j + 1$ through auxiliary layer $j + 1/2$.

Let us consider the transitions between the layers $t_{j+1/2}$ and t_{j+1} for the components of the wind velocity and the excess pressure. We obtain the Poisson equation for function δP

$$\Delta\left(\frac{\delta P}{\rho_0} + \frac{2}{3} E \right) = -\frac{1}{2} \frac{\partial}{\partial t}\left(\frac{\partial u}{\partial x} + \frac{\partial w}{\partial z} \right).$$

We approximate the derivative with respect to time in the right side of this equation by the finite difference. In this case, we find δP at a new layer in time. Since the equation of discontinuity should be fulfilled at the integer layers in time, the expression $\delta \tilde{P}^{j+1} = \left(\frac{\delta P^{j+1}}{\rho_0} + \frac{2}{3} E^j \right)$ should be the solution of the Poisson equation:

$$\Delta \delta \tilde{P}^{j+1} = \frac{1}{\tau}\left(\frac{\partial u^{j+1/2}}{\partial x} + \frac{\partial w^{j+1/2}}{\partial z} \right). \tag{7}$$

Approximating Eq. (7) for the function $\delta \tilde{P}^{j+1}$ and complementing it with the corresponding boundary conditions, we obtain a system of linear algebraic equations that can be solved using the matrix sweep method [30]. When the values of $\delta \tilde{P}_{n,m}^{j+1}$ are found, the components of the wind velocity at the layer $j + 1$ can be calculated by the formulas

$$u_{n,m}^{j+1} = u_{n,m}^{j+1/2} - \tau \frac{\delta \tilde{P}_{n+1,m}^{j+1} - \delta \tilde{P}_{n-1,m}^{j+1}}{x_{n+1} - x_{n-1}},$$

$$w_{n,m}^{j+1} = w_{n,m}^{j+1/2} - \tau \frac{\delta \tilde{P}_{n,m+1}^{j+1} - \delta \tilde{P}_{n,m-1}^{j+1}}{z_{m+1} - z_{m-1}}.$$

To reduce the computational expenses, we use a quasi-homogeneous grid with respect to a vertical coordinate. The system of equations complemented by the initial and boundary conditions is solved using the relaxation (iterative) method.

General Characteristics of Model Experiments

To calculate F_C along the profile selected, we performed two series of experiments using the 2D model. The first model experiment (2D) included the flux calculations taking into account the disturbing influence of the heterogeneous structure of vegetation and surface topography on the wind and turbulence field.

In the second experiment, the selected profile was considered an assemblage of elementary horizontally homogeneous segments, for each of which the vertical fluxes were calculated by the 2D model under the assumption that the horizontal advection within each selected segment is zero (that is possible if the dimension of each selected segment is considered as infinitely large). In this case, we did not examine the influence exerted on the turbulent regime and the processes of CO_2 transfer by the boundary effects, which appear at the boundaries between the vegetation communities with different properties, as well as at topographic irregularities. Thus, to calculate the vertical flows, we imitated a classical approach used for calculating the atmospheric fluxes above the homogeneous ground surface (1D), which implies the dependence of all required functions (wind-velocity components, coefficient of turbulent exchange, etc.) on only one spatial coordinate—the height above the ground surface.

In each experiment, the integral fluxes for the entire profile are calculated by integrating the vertical fluxes obtained for each separate segment.

To identify the maximum possible effect of the surface heterogeneity on the vertical CO_2 fluxes, we selected for our numerical experiments a typical summer day with sunny and warm weather conditions that usually provide the maximum rates of photosynthesis for the forest vegetation and agricultural plants. In our
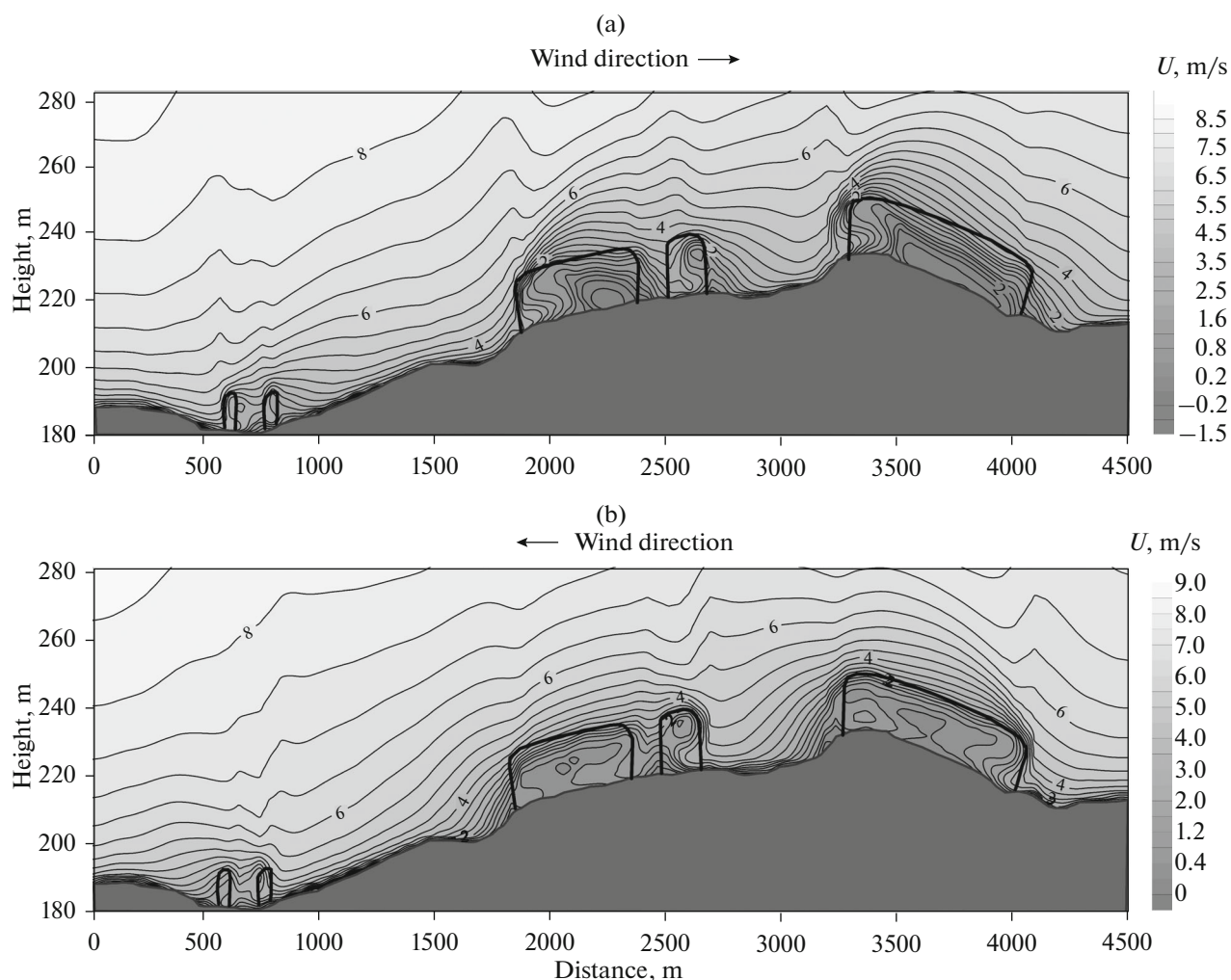
Fig. 2. Calculated vertical cross sections of the horizontal wind component for (a) the prevailing wind direction and (b) the wind of opposite direction. The solid lines designate conventional borders of forest vegetation. The negative values of the wind velocity correspond to the backward wind direction.

calculations, we used the typical values of summer meteorological parameters for this area: an air temperature of +25°C, a relative humidity of 40%, and an incoming solar radiation of 750 W m^{-2}. To minimize the possible effects of shadowing of some ground surface segments by surrounding vegetation communities or topographical irregularities on plant photosynthesis rate, for our experiments we selected the time interval when the sun azimuth was perpendicular to the selected profile. Such sun condition for the selected profile is observed at the forenoon time. The height of the sun taken for the numerical experiments was 60°.

In view of significant horizontal heterogeneity of the surface topography and the vegetation cover in the selected area, we performed model calculations of the wind velocity field, coefficients of turbulence, and vertical fluxes of CO_2 for two main wind directions: the southwest wind direction that is dominant in this

area in the summer time and the opposite northeast direction.

For the model calculations, the grid spacing along the horizontal coordinate x was taken as 10 m. A quasi-uniform grid with a minimal spacing of 0.4 m was used along vertical coordinate z.

RESULTS AND DISCUSSION

The results of the modeling experiments showed that the complex topography and mosaic vegetation cover have a significant influence on the spatial patterns of the wind speed and turbulent exchange coefficient (Figs. 2–3). A typical feature of the calculated fields of wind speed and coefficients of turbulent exchange is the maximum gradients of their change at the windward segments of the slopes and forest edges. The results also indicated circular movements of the air in the downwind side of the obstacles accompanied
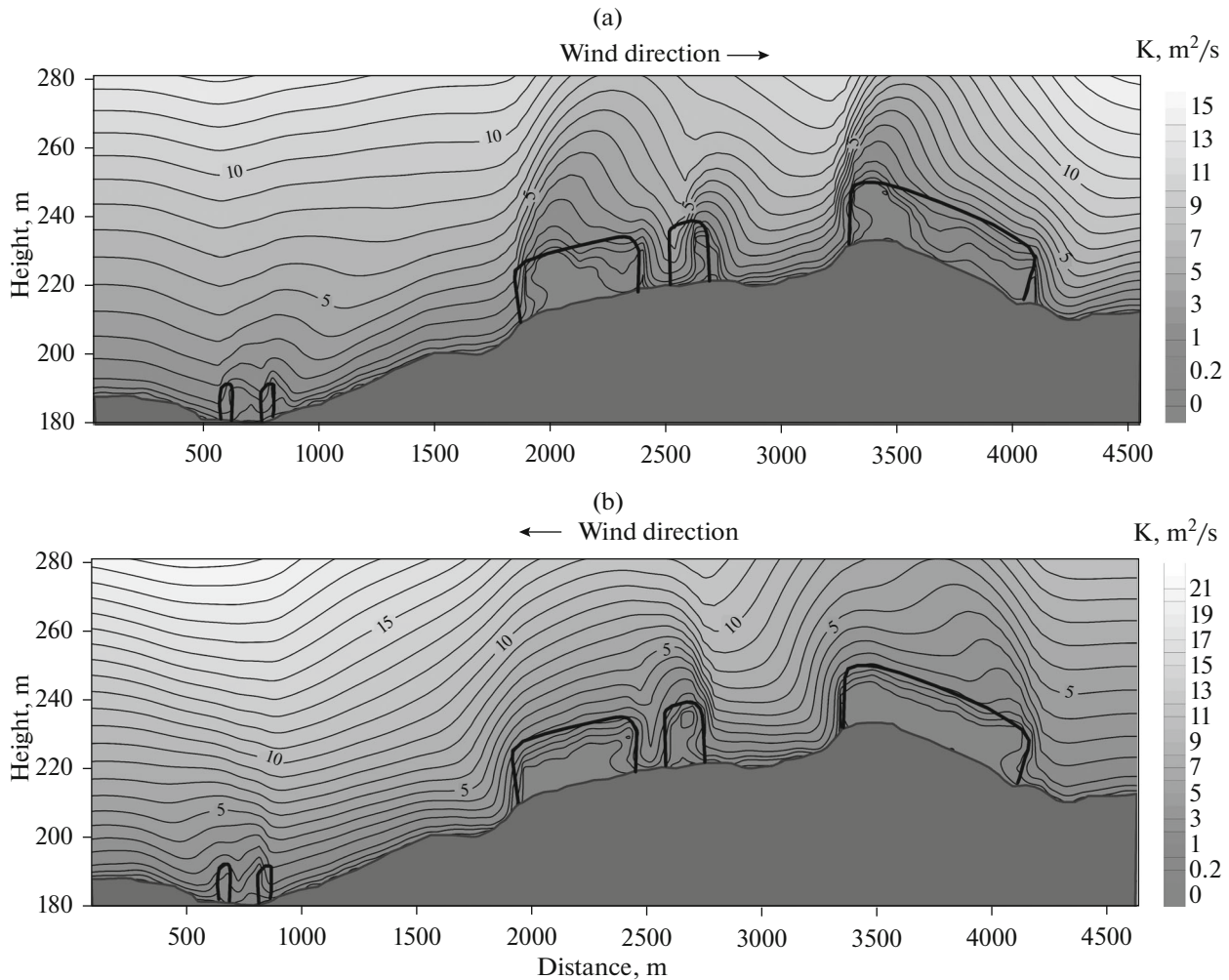
(a)
Wind direction ⟶

(b)
⟵ Wind direction

Fig. 3. Calculated vertical cross-sections of the coefficient of turbulent exchange for (a) the prevailing wind direction and (b) the wind of opposite direction. The solid lines designate conventional borders of forest vegetation.

by air flows directed oppositely to the main wind direction in the atmospheric surface layer.

The vertical CO_2 fluxes calculated along the entire profile at a prevailing southwestern wind direction were characterized by significant variability and ranged from $+5\ \mu mol\ m^{-2}\ s^{-1}$ at the windward sides of the ploughed field to $-32.0\ \mu mol\ m^{-2}\ s^{-1}$ above the forested profile segments (Fig. 4). The "−" sign corresponds to the direction of the CO_2 flux from the atmosphere to the ground surface and the "+" sign corresponds to that from the ground surface to the atmosphere, respectively. Under northeastern wind direction, the maximum CO_2 fluxes towards the surface reached $25\ \mu mol\ m^{-2}\ s^{-1}$. The differences in the fluxes above the similar profile segments are determined primarily by the horizontal advection and the influence of orographic effects.

Upon the dominant southwest direction of the wind, the value of the total CO_2 flux for the entire pro-

file amounted to $-13.9\ \mu mol\ m^{-2}\ s^{-1}$. When the wind direction was northeast, the entire CO_2 flux under similar solar radiation and air temperature conditions was somewhat smaller and equaled $-11.5\ \mu mol\ m^{-2}\ s^{-1}$.

During the second experiment (when CO_2 fluxes were calculated for the scenario imitating a 1D model approach), the calculated values of the CO_2 fluxes above the different profile segments with various types of land use varied from $+4.9\ \mu mol\ m^{-2}\ s^{-1}$ above the new-ploughed field to $-5.4\ \mu mol\ m^{-2}\ s^{-1}$ above the agricultural crops and meadow vegetation and to $-23.5\ \mu mol\ m^{-2}\ s^{-1}$ above the forest areas (Fig. 4). In view of the total length of the cross-section segments with a different structure of land use (12% of ploughed field, 8% of meadow vegetation, 48% of agricultural plants, and 32% of forest area), the mean CO_2 fluxes for the entire profile were $-10.2\ \mu mol\ m^{-2}\ s^{-1}$.

Thus, the total CO_2 uptake by the ground surface along the profile obtained during the second experi-
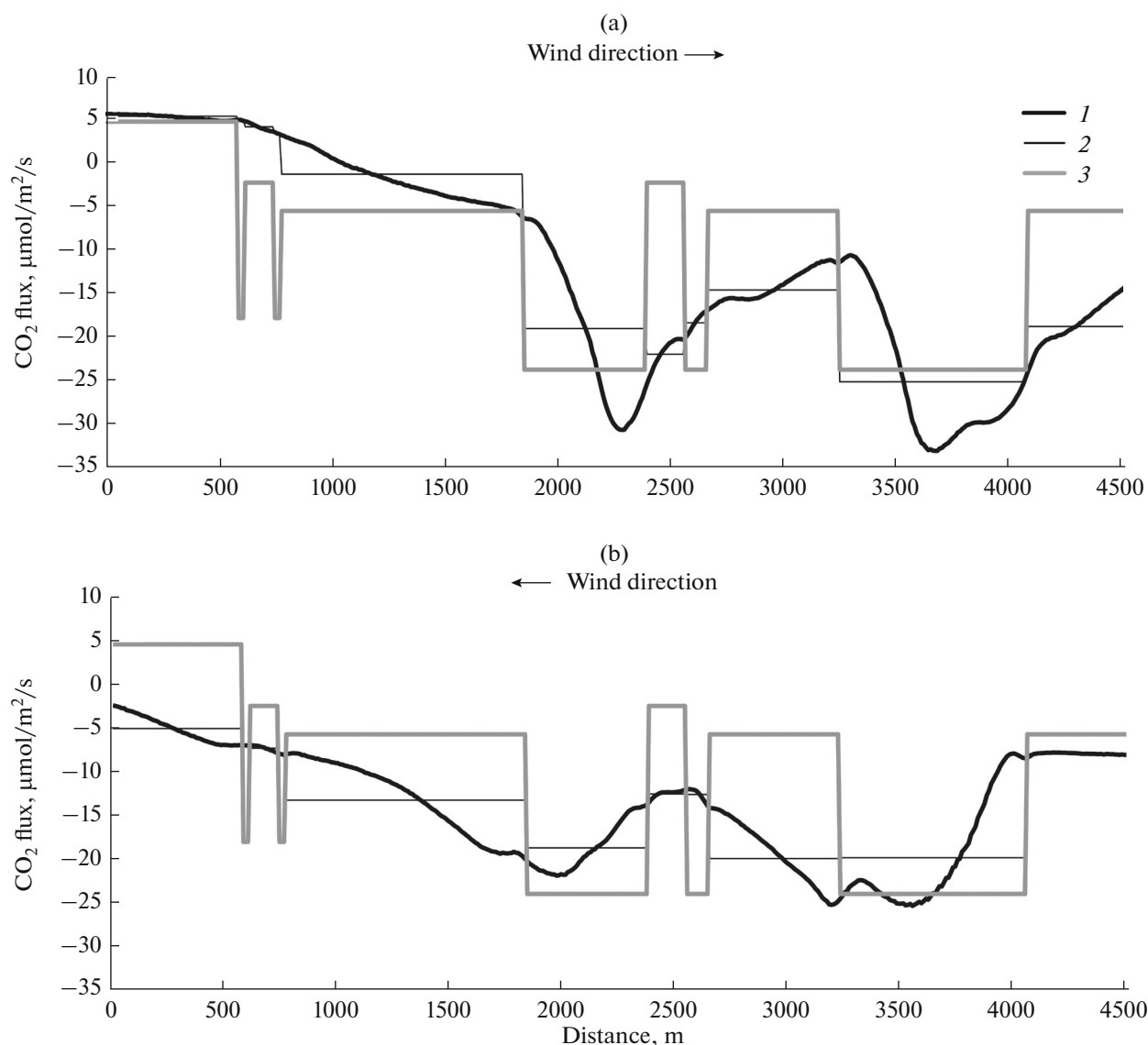
Fig. 4. Calculated vertical CO_2 fluxes at a height of 40 m above the ground surface along the profile for (a) the prevailing wind direction and (b) wind of the opposite direction. The fluxes are modeled using two scenarios (1D and 2D).
(*1*) is the vertical flux calculated using the 2D model for the first model scenario; (*2*) is the vertical CO_2 fluxes calculated for the first model scenario and averaged for each homogeneous segment of the selected profile; (*3*) is the vertical CO_2 fluxes calculated using a 2D model for the second model scenario and assumed that the horizontal advection is zero (imitation of a 1D approach).

ment turned out to be 26% less than the CO_2 uptake by the ground surface obtained in the first experiment under southwestern wind and 11% less − under northeastern wind direction, respectively.

The differences in the integral values of CO_2 fluxes calculated for the entire profile are evidently determined by the spatial heterogeneity of the wind field and the coefficients of turbulent exchange in the atmospheric surface layer, due to the heterogeneous structure of vegetation and the complex topography. It may result in the different rates of CO_2 emission from the soil surface at the different segments of the profile under study. In addition, some differences can be

caused by the used boundary conditions, as well as by the contribution of horizontal advection of CO_2 between the segments of the profile with a different land use structure. We need to take into account that during the experiments it was assumed that the sun azimuth was perpendicular to the main direction of the profile selected. The change in the sun azimuth and the light conditions can evidently lead to more significant differences in the fluxes being modeled for the other time intervals.

We should also bear in mind that the accuracy of our calculations is limited by several factors, primarily by the model approximation used to describe CO_2

emission from the soil surface as a function of the wind velocity, by the approximation used in solving the system of equations based on the 1.5th order closure, the use of the Boussinesq hypothesis, and the expression of coefficients of turbulent diffusion through the turbulence kinetic energy and the rate of its dissipation. The errors determined in the calculations appear in solving the system of equations using the selected difference scheme. The error level is also affected by the accuracy of assigning the boundary conditions.

To estimate the calculation errors that appear in solving the system of differential equations, we analyzed the results of the flux calculations for different heights above the ground surface, provided for the second model experiment when the influence of vegetation and topography heterogeneity on atmospheric fluxes was ignored. In the ideal case, the rates of the CO_2 flux must be equal at different heights above the surface under such conditions. However, the modeling results showed that the calculated values of the CO_2 fluxes are not the same and slightly varied at different heights. The standard deviation that characterizes the spread in the values was ± 0.65 μmol m^{-2} s^{-1} at a standard calculation error of ± 0.28 μmol m^{-2} s^{-1}. Thus, the calculation errors were significantly lower than the differences between the modeled fluxes, which were obtained during the first and second model experiments. This can serve as a good indicator to confirm the reliability of the model estimates.

CONCLUSIONS

The results of CO_2 flux calculation using the 2D process-based model along the 4.5 km profile with a complex topography and heterogeneous vegetation showed a significant influence exerted by the land surface heterogeneity on the turbulent transfer of CO_2 within the atmospheric surface layer. The integral vertical fluxes calculated during the second model experiment that considered the heterogeneous surface profile as an assemblage of independent horizontally homogeneous segments with specific structures and properties were steadily lower with respect to the absolute flux values for the selected weather conditions than the values of the CO_2 fluxes calculated during the first experiment that took into account the real spatial patterns of wind speed and turbulent exchange coefficients above the considered non-uniform land surface. The identified differences are related mostly with the overestimation of the wind velocity and the turbulent exchange rate in the air layer near the soil surface and, as a rule, with the overestimated contribution of the CO_2 emission from the soil surface to the total ecosystem fluxes of CO_2 in the model experiment that ignores the influence of the horizontal surface heterogeneity on the spatial wind distribution, and which is conventionally used in 1D models. The differences between the average CO_2 flux calculated for the entire profile at a

height of 40 m above the ground surface varied from 11 to 26%, depending on the wind direction and the related changes in the contribution of different land use types into total atmospheric CO_2 fluxes.

Thus, the results of our study indicate the importance of a quantitative estimation of the influence exerted by spatial heterogeneity of the land surface with a mosaic structure of vegetation and complex topography on the turbulence and wind fields, as well as on the processes of transfer within the atmospheric surface layer. If horizontal heterogeneity is neglected during the calculations of vertical fluxes, significant errors can occur even at quite large surface segments in the calculations of CO_2 fluxes between the land surface and the atmosphere, even when someone uses quite detailed 1D process-based models.

REFERENCES

1. L. R. Tsvang, "Measurements of spectra of temperature pulsations in the free atmosphere," Izv. Akad. Nauk SSSR: Geofiz., No. 11, 1674−1678 (1960).

2. L. G. Elagina and A. I. Lazarev, "Measurements of frequency pulsations of CO_2 in the atmospheric surface layer," Izv. Akad. Nauk SSSR: Fiz. Atmos. Okeana **20** (6), 536−540 (1984).

3. T. Foken, *Micrometeorology* (Springer, Heidelberg, 2008).

4. G. E. Insarov, O. K. Borisova, M. D. Korzukhin, et al., "Natural land ecosystems," in *Methods for the Assessment of Climate Change Consequences for Physical and Biological Systems*, Ed. by S. M. Semenov (Planeta, Moscow, 2012), pp. 190−265 [in Russian].

5. G. G. Burba, Yu. A. Kurbatova, O. A. Kuricheva, et al., *The Method of Turbulent Pulsations: A Brief Guidance Manual* (LI-COR Biosciences, IPEE RAN, 2016) [in Russian].

6. P. Sellers, R. E. Dickinson, D. A. Randall, et al., "Modeling the exchanges of energy, water, and carbon between continents and the atmosphere," Science **275**, 502−509 (1997).

7. A. Oltchev, J. Cermak, N. Nadezhdina, et al., "Transpiration of a mixed forest stand: Field measurements and simulation using SVAT models," Boreal Environ. Res. **7** (4), 389−397 (2002).

8. E. M. Gusev and O. N. Nasonova, *Modeling of Heat and Moisture Exchange of Land Surface with the Atmosphere* (Nauka, Moscow, 2010) [in Russian].

9. A. S. Monin, Theoretical Foundations of Geophysical Hydrodynamics (Gidrometeoizdat, Leningrad, 1988) [in Russian].

10. N. L. Byzova, V. N. Ivanov, and E. K. Garger, *Turbulence in the Atmospheric Boundary Layer* (Gidrometeoizdat, Leningrad, 1989) [in Russian].

11. M. G. Boyarshinov and V. D. Goremykin, "Spatial model of airflow interaction with vegetation," Mat. Model. **16** (7), 31−42 (2004).

12. M. G. Boyarshinov and D. S. Balabanov, "Pollution of the atmospheric air of a city quarter by point-source exhaust gases," Mat. Model. **26** (4), 97−109 (2013).

13. R. Pielke, *Mesoscale Meteorological Modelling* (Academic, San Diego, 2002).

14. S. S. Zilitinkevich, *Dynamics of Atmospheric Boundary Layer* (Gidrometeoizdat, Leningrad, 1970) [in Russian].

15. J. R. Garratt, *The Atmospheric Boundary Layer* (Cambridge University Press, Cambridge, UK, 1992).

16. N. T. Levashova, J. V. Mukhartova, M. A. Davydova, N. E. Shapkina, and A. V. Oltchev, "The application of the theory of contrast structures for describing wind field in spatially heterogeneous vegetation cover," Moscow Univ. Phys. Bull. **70** (3), 167−174 (2015).

17. J. V. Mukhartova, N. T. Levashova, A. V. Olchev, et al., "Application of a 2D model for describing the turbulent transfer of CO_2 in a spatially heterogeneous vegetation cover," Moscow Univ. Phys. Bull. **70** (1), 14−21 (2015).

18. A. S. Dubov, L. P. Bykova, and S. V. Marunich, *Turbulence in the Vegetation Cover* (Gidrometeoizdat, Leningrad, 1978) [in Russian].

19. A. Sogachev and O. Panferov, "Modification of two-equation models to account for plant drag," Boundary-Layer Meteorol. **121** (2), 229−266 (2006).

20. D. C. Wilcox, *Turbulence modeling for CFD* (DCW Industries, La Canada, 1998).

21. A. Olchev, K. Radler, A. Sogachev, et al., "Application of a three-dimensional model for assessing effects of small clear-cuttings on radiation and soil temperature," J. Ecol. Modell. **220**, 3046−3056 (2009).

22. R. B. Stull, *An Introduction to Boundary Layer Meteorology* (Kluwer, Dordrecht, 1988).

23. T. K. Flesch, J. H. Prueger, and J. L. Hatfield, "Turbulent Schmidt number from a tracer experiment," Agric. For. Meteorol. **111**, 299−307 (2002).

24. J. T. Ball, I. E. Woodrow, and J. A. Berry, "A model predicting stomatal conductance and its contribution to the control of photosynthesis under different environmental conditions," in *Progress in Photosynthesis Research*, Ed. by I. Biggins (Martinus Nijhoff, Netherlands, 1987), pp. 221−224.

25. R. Leuning, "A critical appraisal of a combined stomatal-photosynthesis model for C_3 plants," Plant Cell Environ. **18**, 339−355 (1995).

26. A. Oltchev, J. Constantin, G. Gravenhorst, et al., "Application of a six-layer SVAT model for simulation of evapotranspiration and water uptake in a spruce forest," J. Phys. Chem. Earth **21** (3), 195−199 (1996).

27. A. Olchev, E. Volkova, T. Karataeva, et al., "Growing season variability of net ecosystem CO_2 exchange and evapotranspiration of a sphagnum mire in the broad-leaved forest zone of European Russia," Environ. Res. Lett. **8** (3), 035051 (2013).

28. B. E. Medlyn, E. Dreyer, D. Ellsworth, et al., "Temperature response of parameters of a biochemically based model of photosynthesis. II. A review of experimental data," Plant Cell Environ. **25**, 1167−1179 (2002).

29. O. M. Belotserkovskii, *Numerical Modeling in Mechanics of Continuous Media* (Fizmatlit, Moscow, 1994) [in Russian].

30. A. A. Samarskii, *Theory of Difference Schemes* (Nauka, Moscow, 1977) [in Russian].

31. N. N. Kalitkin and P. V. Karyakin, *Numerical Methods*, Vol. 2: *Methods of Mathematical Physics* (Akademiya, Moscow, 2013) [in Russian].

Translated by L. Mukhortova